Astrophysical S factor for the ^{6}Li$(d,\alpha)^4$He and ^{6}Li$(d, p_0/p_1)^7$Li reactions and their astrophysical implications

Kaihong Fang,[1,2,*] Jianxin Zou,[1] Houjun He,[1] Qiang Wang,[1] Jiangtao Zhao,[1] Tieshan Wang,[1] and Jirohta Kasagi[2]

[1]*School of Nuclear Science and Technology, Lanzhou University, Lanzhou, Gansu Province 730000, People's Republic of China*

[2]*Research Center for Electron Photon Science, Tohoku University, Sendai 982-0826, Japan*

In this work, three astrophysical $S(E)$ factors of the ^{6}Li$(d,\alpha)^4$He, ^{6}Li$(d, p_0)^7$Li, and ^{6}Li$(d, p_1)^7$Li* reactions have been presented, and the value of screening potential was also deduced, where the subsequent two $S(E)$ factors were reported for the first time. The present extracted astrophysical $S(E)$ factors result in $S_{\text{bare}}(0) = 19.20 \pm 0.52, 20.46 \pm 0.63$, and 3.79 ± 0.18 MeV b for the ^{6}Li$(d,\alpha)^4$He, ^{6}Li$(d, p_0)^7$Li, and ^{6}Li$(d, p_1)^7$Li* reactions, respectively. The deduced screening potential (U_s) is 478 ± 42 eV in the liquid lithium ($\sim$530 K) host which is much larger than the expected value of 186 eV calculated by adiabatic approximation. Using these results, the stellar reaction rates for the ^{6}Li$(d,\alpha)^4$He and ^{6}Li$(d, p_0 + p_1)^7$Li reactions for temperatures up to $T = 3 \times 10^9$K were calculated, so as to estimate the abundances of ^{6}Li and ^{7}Li in the solar proton-proton burning process.

I. INTRODUCTION

As the mechanism of producing elements in the universe, charged-particle induced reactions at energies of astrophysical interest has long been the subject of theoretical and experimental investigation. It can be seen that nucleosynthesis in big-bang and stellar interiors can account for nearly all the elements of the periodic table, however, both production and depletion mechanisms of lithium isotopes are the astrophysical problems which are still not completely solved until now, namely the amount of lithium (^{6}Li and ^{7}Li) predicted by the standard big-bang nucleosynthesis (BBN) is in conflict with observations [1–6]. There is no doubt that lithium destruction plays an important role in the problem of abundance of lithium either in the sun or in other main sequence (MS) stars making up the various galactic populations [7]. Though lithium destruction could be enhanced by unknown or poorly measured resonances [4], nuclear physics experiments provide a wealth of significative cross section data.

However, as it usually happens for charged-particle induced reactions, at the interested energies far below the Coulomb barrier, the cross section [$\sigma(E)$] drops steeply (nearly exponentially) as energy E decreases. Thus, the direct measurement of $\sigma(E)$ at the thermonuclear energy becomes almost impossible. Instead, the measured energy dependence of $\sigma(E)$ at higher energies must be extrapolated to stellar energies. Generally, it is advantageous to transform the $\sigma(E)$ into the astrophysical $S(E)$ factor, defined by the relation [2]

$$\sigma(E) = S(E)E^{-1}\exp(-2\pi\eta(E)), \tag{1}$$

where E is the reaction energy in the center-of-mass (c.m.) system, and $\eta(E) = Z_1 Z_2 \alpha(\mu c^2/2E)^{1/2}$ is the corresponding Sommerfeld parameter (Z_1 and Z_2 are atomic numbers of the target and projectile, α is the fine structure constant, μ is the reduced mass in amu, and c is velocity of light). Different from $\sigma(E)$, $S(E)$ which contains all nuclear effects

[8] varies smoothly with energy E for nonresonant reactions. Commonly, $S(E)$ in the low-energy region can be extrapolated according to the trend of experimental data in the high-energy region.

In Eq. (1), it is assumed that the Coulomb potential between the target nucleus and projectile is that resulting from bare nuclei. However, in laboratory measurements, the target nuclei and the projectiles are in the form of neutral atoms/molecules and ions, respectively, thus the Coulomb field would be screened by the charges surrounding the interacting nuclei. The effect of these screening charges is to increase the penetrability through the Coulomb barrier and thus to enhance the cross section [or equivalently the $S(E)$ factor]. The corresponding enhancement ratio [$S(E)/S_{\text{bare}}(E)$] can be defined by the equation [9]

$$f(E) = \frac{E}{(E + U_s)}\exp\left(\pi\eta\frac{U_s}{E}\right), \tag{2}$$

where U_s is the screening potential (assumed to be constant) which depends on the bound /free electrons [10,11] or free ions [12,13] surrounding the interacting nuclei. Note that $f(E)$ increases exponentially as the incident energy decreases. For energy ratios $E/U_s \geqslant 1000$, $f(E)$ is almost 1, so laboratory experiments can be regarded as essentially measuring $\sigma_{\text{bare}}(E)$. It should be pointed out that, in the astrophysical environments, the cross section under plasma conditions $\sigma_{el}(E)$ is related to the bare cross section $\sigma_{\text{bare}}(E)$ multiplied by a similar enhancement factor which depends on detailed properties of the plasma, such as the Debye-Hückel radius [7].

In the past few decades, many researchers have studied the reactions related to destruction mechanisms for lithium [14–21]. Engstler *et al.* [15] measured the cross sections of the ^{7}Li$(p,\alpha)^4$He, ^{6}Li$(d,\alpha)^4$He, and ^{6}Li$(p,\alpha)^3$He reactions involving the use of normal kinematics with hydrogen projectiles and LiF solid targets as well as inverse kinematics with Li$^+$ projectiles and hydrogen molecular gas targets over the c.m. energy range of $E = 10$–1450 keV. All these derived values of U_s are significantly larger than the value of 186 eV estimated from adiabatic approximation [22]. Wang *et al.* [14]

*fangkh@lzu.edu.cn

and Barker [16] have reanalyzed the same experimental data obtained by Engstler *et al.* [15], and gave different results. Actually, $^6\mathrm{Li}(d,p)^7\mathrm{Li}$ reaction contains two reaction channels, $^6\mathrm{Li}(d,p_0)^7\mathrm{Li}$ ($Q = 5.03$ MeV) and $^6\mathrm{Li}(d,p_1)^7\mathrm{Li}^*$ ($Q = 4.55$ MeV). For the two reactions channels, related studies mainly concentrated in the cross section measurement, but reports involved with astrophysical S factor are not enough, especially in the low-energy region. Elwyn *et al.* [23] measured the total reaction cross sections and differential cross sections for $(d,n),(d,p)$, and (d,α) reactions initiated by $\sim$0.1 to $\sim$1.0 MeV deuterons on $^6\mathrm{Li}$ with absolute accuracies of 8–13%. Czerski *et al.* [21] studied the two reactions for the relevant deuteron energies $E =$ 65–135 keV and 90–180 keV, respectively. By analyzing the cross section values obtained by Elwyn *et al.* [23], Czerski *et al.* gave the astrophysical S-factor curves (no specific parameters) for the $^6\mathrm{Li}(d,p_0)^7\mathrm{Li}$ and $^6\mathrm{Li}(d,p_1)^7\mathrm{Li}^*$ reactions.

Due to the difficulties encountered in charged-particle experimental studies at sub-Coulomb energies (e.g., electron screening effect), the Trojan-horse method (THM) [24], which is considered to determine the astrophysical $S(E)$ factor independent from the screening energy, has been applied to extract relative values of the astrophysical $S_{\mathrm{bare}}(E)$ factor for the $^6\mathrm{Li}(d,\alpha)^4\mathrm{He}$, $^7\mathrm{Li}(p,\alpha)^4\mathrm{He}$, and $^6\mathrm{Li}(p,\alpha)^3\mathrm{He}$ reactions [18–20]. So far, THM has been considered to be a very effective method to extract the relative $S_{\mathrm{bare}}(E)$ factor in the low-energy region.

Different from other authors mentioned above, Pizzone *et al.* [7,18] used their own results for $^6\mathrm{Li}(p,\alpha)^3\mathrm{He}$ and $^7\mathrm{Li}(p,\alpha)^4\mathrm{He}$ reactions to simulate the lithium abundance on the solar surface. According to the simulation results, they concluded that the problem of the surface lithium abundances is not at the nuclear physics level and the solution of the problem of light elements destruction in stars lies elsewhere. In the present work, in order to study more details about the reactions involving lithium ($^6\mathrm{Li}$) isotope related to the astrophysical application, we employed the liquid enriched $^6\mathrm{Li}$ for the $^6\mathrm{Li}(d,\alpha)^4\mathrm{He}$, $^6\mathrm{Li}(d,p_0)^7\mathrm{Li}$, and $^6\mathrm{Li}(d,p_1)^7\mathrm{Li}^*$ reactions measurement so as to deduce the astrophysical $S_{\mathrm{bare}}(E)$ factors and U_s provided by surrounding charges, simultaneously. The deduced $S_{\mathrm{bare}}(E)$ factor was a parametrized cubic polynomial expressed as $S_{\mathrm{bare}}(E) = a + bE + cE^2 + dE^3$. For the astrophysical application, the stellar reaction rates for the $^6\mathrm{Li}(d,\alpha)^4\mathrm{He}$ and $^6\mathrm{Li}(d,p_0 + p_1)^7\mathrm{Li}$ reactions were determined, and the lithium abundance in solar proton-proton burning was simulated also. More details will be shown in the following sections.

II. EXPERIMENTAL PROCEDURE

The experiment was performed by using a low-energy high-current ion beam generator at the Research Center for Electron Photon Science of Tohoku University, details of which were reported in refs. [25,26]. In this work, we measured the thick-target yields of particles emitted from the $^6\mathrm{Li}(d,\alpha)^4\mathrm{He}$ and $^6\mathrm{Li}(d,p)^7\mathrm{Li}$ reactions in the deuteron energy range from 30 to 70 keV by 2.5-keV steps, occurring in liquid Li ($T \sim 530$ K) medium.

The deuteron beam, which was bent by an angle of 60° with respect to the horizontal plane, irradiated the lithium target surface after passing through an aperture determining the beam size ($\sim$5 mm diameter). Two Si surface barrier detectors (an angle of 125° with respect to the beam direction, 300 μm in thickness and 450 mm^2 in area) were used to detect the emitted charged particles, with a total solid angle ($\Delta\Omega/4\pi$) of about 5.0%. A thin Al foil (5 μm thick) was placed in the front of each detector to prevent scattered particles from hitting the detector directly. In order to avoid being heated by thermal emissions from the high temperature target, the detector holder was cooled by water at 5 °C. The liquid $^6\mathrm{Li}$ target (enrichment of 95%) was in an open container which was placed horizontally at the center of the chamber with pressure about 9×10^{-4} Pa.

As an active element, lithium easily reacts with other materials (other than inert gas), thus much attention should be paid to the preparation and cleanness of the target during the bombardment. The pure-liquid-Li sample was prepared in a glove box (filled with argon gas) connecting with the chamber. During the experiment, the lithium target was easily covered with compounds such as LiD or $\mathrm{Li_2O}$, so it was necessary to monitor and clean the Li target surface. Two methods were used to monitor the surface condition: (1) the real-time output data of the radiation thermometer (R.T.), which was used to monitor the temperature of the Li surface, would fluctuate anomalously with any contamination floating on the surface; (2) the yield of proton from the $D(d,p)T$ reaction would increase strongly if the surface was deteriorated by the implanted deuterium. In the cleaning process, we used the sharp scraper to make contact with the liquid Li surface gently, making the solid contamination adsorb to the blade surface.

The beam energy (E_d) was from 30 to 70 keV by 2.5-keV steps with the energy uncertainty smaller than 30 eV. Considering the potential influence of temperature on screening effect (in fact, we have measured this influence [27]), we kept the same beam power (500 mW) during the experiment to maintain the target conditions as similarly as possible. More details about that experiment can be found in Refs. [27,28].

III. EXPERIMENTAL RESULTS

The emitted charged-particles spectra measured at 70, 50, and 30 keV are illustrated in Fig. 1. Four peaks corresponding to protons (p) from the $D(d,p)t$ reaction, protons (p_1 and p_0) from the $^6\mathrm{Li}(d,p_1/p_0)^7\mathrm{Li}$ reactions, and α particles from the $^6\mathrm{Li}(d,\alpha)^4\mathrm{He}$ reaction are indicated, respectively. The continuous events below 1000 channels originate from the $^7\mathrm{Li}(d,\alpha)n^4\mathrm{He}$ reaction due to the residual $^7\mathrm{Li}$ (5%) in the enriched $^6\mathrm{Li}$ target.

The key observation objects ($E_{\mathrm{p1}} = 3.9$ MeV, $E_{\mathrm{p0}} = 4.3$ MeV, and $E_\alpha = 10.9$ MeV) are clearly identified. Due to the low bombarding energy (30–70 keV with 2.5-keV steps), the peaks of objective particles with a very wide dynamic range (up to 10 MeV) seem identical, with an inconspicuous energy shift. In low-beam-energy spectra, the p peak from the $D(d,p)T$ reaction seems to be enhanced
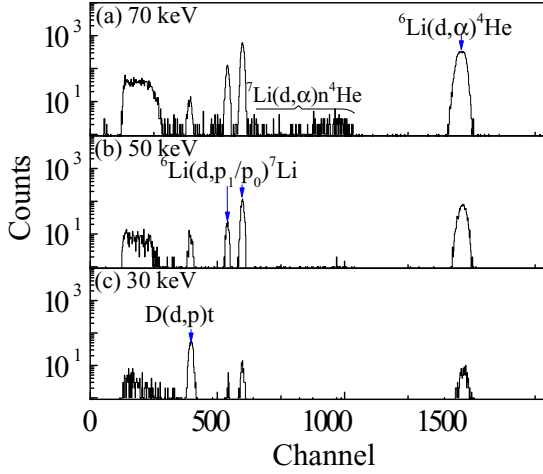
FIG. 1. Charged-particle spectra for the (a) 70-, (b) 50-, and (c) 30-keV deuteron bombardments on liquid enriched ^{6}Li target, respectively. Four peaks, protons (p) from the $D(d,p)t$ reaction, protons (p_1 and p_0) from the ^{6}Li$(d,p_1/p_0)^7$Li reactions, and α particles from the ^{6}Li$(d,\alpha)^4$He reaction, are indicated.

compared with the weakened α peak, that is because the decreased rate of the d-^{6}Li reaction cross section is much greater than that of d-D reaction. Meanwhile, the continuous events from d-^{7}Li reaction below 1000 channels would accumulate the counts of p_0 and p_1 peaks as a "background". When approximately estimating a uniform distribution (from 3.6 to 4.6 MeV region [29]), the counting rate of $p_1(p_0)$ to α events was less than 2% (0.4%) which should be deducted.

Figure 2 shows the obtained thick-target yields of the ^{6}Li$(d,p_1/p_0)^7$Li and ^{6}Li$(d,\alpha)^4$He reactions measured from 30 to 70 keV with unit counts per μC of the incident deuteron. The thick-target α yield [$Y_\alpha^{\text{thick}}(E_d)$] is essentially an energy integral of the cross section divided by the stopping power of the beam particle; for the projectile energy E_p (in laboratory
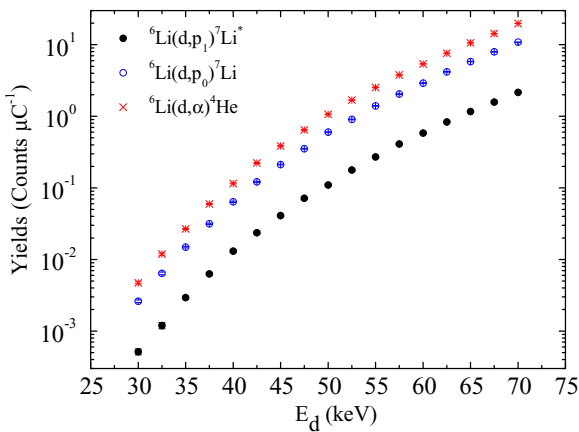

FIG. 2. Thick-target yields of charged particles emitted from the ^{6}Li$(d,p_1/p_0)^7$Li and ^{6}Li$(d,\alpha)^4$He reactions as a function of the bombarding energy of deuterons.

system), it is expressed as

$$Y_\alpha^{\text{thick}}(E_p) = 2\frac{0.95 N_d N_t \Delta\Omega_{\text{lab}}}{4\pi} \int_0^{E_p} \frac{d\Omega_{\text{c.m.}}}{d\Omega_{\text{lab}}} \sigma(E_{\text{c.m.}}, U_s)$$

$$\times \left(\frac{dE}{dx}\right)^{-1} dE$$

$$= 2\frac{0.95 N_d N_t \Delta\Omega_{\text{lab}}}{4\pi} \int_0^{E_p} \frac{d\Omega_{\text{c.m.}}}{d\Omega_{\text{lab}}} \frac{S(E_{\text{c.m.}})}{E_{\text{c.m.}}}$$

$$\times \exp(-2\pi\eta(E_{\text{c.m.}} + U_s)) \times \left(\frac{dE}{dx}\right)^{-1} dE \quad (3)$$

where N_d is the number of incident deuterons, N_t is the number density of target atoms, 0.95 is the enrichment of ^{6}Li, $\Delta\Omega_{\text{lab}}$ is the solid angle, $d\Omega_{\text{c.m.}}/d\Omega_{\text{lab}}$ is the solid angle ratio of the c.m. to lab system, $S(E_{\text{c.m.}})$ is the astrophysical factor as a function of the c.m. system energy ($E_{\text{c.m.}}$), U_s is the screening potential, and $(dE/dx)^{-1}$ is the stopping power of liquid lithium target (at 530 K) obtained from the SRIM code [30] and multiplied by a correction factor [27]. For ^{6}Li$(d,p_1/p_0)^7$Li reactions, the thick-target proton yield [$Y_p^{\text{thick}}(E_d)$] has a nearly identical expression; just remove the coefficient of 2.

Thus, using the least square method, the screening energies (U_s) provided by the same liquid lithium environment for each reaction channel can be deduced with the aid of reported $S(E)$ curves in Ref. [15] for ^{6}Li$(d,\alpha)^4$He, Ref. [21] for ^{6}Li$(d,p_1)^7$Li, and Ref. [21] for ^{6}Li$(d,p_0)^7$Li. However, the values of U_s show an abnormal disagreement that $U_s = 577 \pm 71$ eV for the ^{6}Li$(d,\alpha)^4$He reaction, $U_s = 152 \pm 55$ eV for the ^{6}Li$(d,p_1)^7$Li reaction, and $U_s = 400 \pm 67$ eV for the ^{6}Li$(d,p_0)^7$Li reaction. That is obviously unacceptable due to the common sense that the same surrounding charges for the d-^{6}Li interaction partners should provide the same screening effect. One may find that the key problem is the rationality of parametrized low-energy $S(E)$ curves which were extrapolated from high-energy measurements. In order to get more self-consistent results, i.e., a uniform screening energy and wide dynamic range practicable $S(E)$ curves, it is a benefit to give a combined fitting of present low-energy data and literature high-energy data. Thus, in the following sections we would discuss the combined data set along this line of thought.

Generally, considering the difficulties of the thin target in the practical application, the thin target yield can be deduced from the two thick-target yields of adjacent energies. In this process, $S(E_{\text{c.m.}})$ is considered as constant over energy step (in this work $\Delta E = 2.5$ keV), thus the thin-target yield (i.e., for α particle) can be obtained by the following equation:

$$Y_\alpha^{\text{thin}}(E_0) = 2\frac{0.95 N_d N_t \Delta\Omega_{\text{lab}}}{4\pi} S(E_{\text{eff}}) \int_{E_0-\Delta}^{E_0} \frac{d\Omega_{\text{c.m.}}}{d\Omega_{\text{lab}}} \frac{1}{E_{\text{c.m.}}}$$

$$\times \exp(-2\pi\eta(E_{\text{c.m.}} + U_s)) \times \left(\frac{dE}{dx}\right)^{-1} dE, \quad (4)$$

where E_{eff} is the effective beam energy, which can be approximated from E_0, Δ, and cross section σ_1 at E_0 and σ_2 at $E_0-\Delta$ [2]. In fact, the astrophysical factor is not a constant within the scope of the energy step (2.5 keV), so it would be
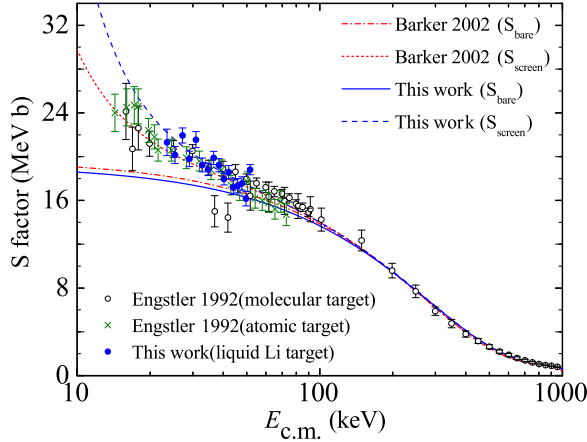
FIG. 3. S factor for the ^{6}Li$(d,\alpha)^4$He reaction as a function of c.m. energy. The solid circles are obtained by thin-target yield. The open circles and crosses are the experimental data for molecular target and atomic target from Engstler 1992 [15]. The dashed and short dashed curves representing the S factor include screening potential contribution of this work and Barker 2002 [16]. The solid and dashed-dotted curves are the corresponding and bare S factors, respectively.

difficult to get accurate results by the thin-target yield, though we calculated the S factor through this method as illustrated in Figs. 3–5.

Based on the reason mentioned above, to avoid introducing additional uncertainties of thin-target yields, the thick-target yields were fitted by using Eq. (3) directly, with the least square method, i.e., Eq. (5a). In the fitting process, each reaction with their corresponding $S_{\text{bare}}(E)$ factor [expressed as $S_{\text{bare}}(E) = a + bE + cE^2 + dE^3$] has four parameters needing to be optimized. Meanwhile, there is a common screening potential [U_s in Eq. (3)] for the three reactions due to the nonisotope
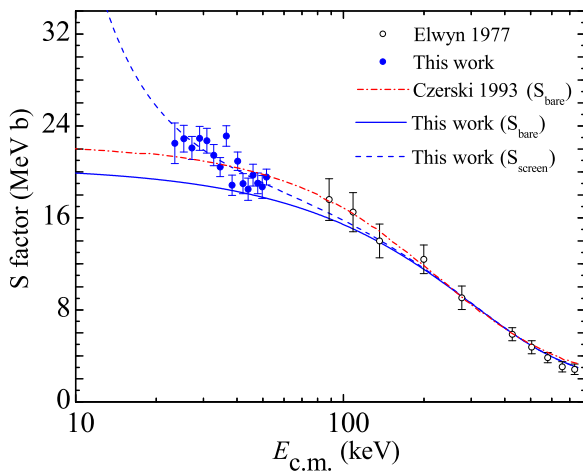

FIG. 4. S factor for the ^{6}Li$(d,p_0)^7$Li reaction as a function of c.m. energy. The solid circles are obtained by thin-target yield. The open circles are the experimental data obtained by Elwyn 1977 [23]. The dashed curve represents the S factor taking screening potential contribution into account, and the solid curve is the corresponding bare S factor. The dashed-dotted curve shows the result estimated from Czerski 1993 [21].
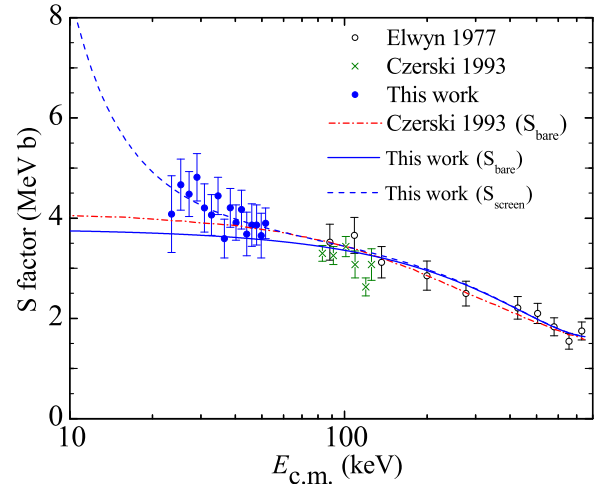

FIG. 5. S factor for the ^{6}Li$(d,p_1)^7$Li* reaction as a function of c.m. energy. The crosses are the experimental data obtained by Czerski 1993 [21]. The rest of the descriptions are the same as in Fig. 4.

dependence effect [15]. Considering the uncertainties in the experimental procedure, a parameter (A) is introduced as a common normalization factor, thus the fitting expression of the thick-target yield, e.g., for the ^{6}Li$(d,\alpha)^4$He reaction, is expressed as $Y_\alpha^{\text{fit}}(E_p) = A \times Y_\alpha^{\text{thick}}(E_p, U_s)$ (ideally, $A = 1$),

$$\chi^2 = \sum \frac{[Y_{\exp}(E_i) - Y_{\text{fit}}(E_i)]^2}{[\Delta Y_{\exp}(E_i)]^2}, \tag{5a}$$

where $\Delta Y_{\exp}(E_i)$ is the statistical uncertainty of experimental yield.

Simultaneously, the present data are concentrated in the low-energy region (30–70 keV), thus the deduced $S(E)$-factor function should be combined with the reported $S_{\exp}(E)$ points in the high-energy region. The reference data are listed below: the data of Engstler *et al.* [15] at $E = 399.6$–952.0 keV (12 points) for the ^{6}Li$(d,\alpha)^4$He reaction, the data of Elwyn *et al.* [23] at $E = 570$–975 keV (five points) for the ^{6}Li$(d,p_0)^7$Li reaction, and the data of Elwyn *et al.* [23] at $E = 570$–975 keV (five points) for the ^{6}Li$(d,p_1)^7$Li* reaction. It should be noted that the experimental data from Engstler *et al.* were multiplied by a normalization factor $k = 0.93$ [15], but our previous work reanalyzed their data and gave a more reasonable result, i.e., $k = 0.95$ [14] which was used in this work.

In other words, we "borrowed" three groups of experimental data [$S_{\exp}(E_i)$] ^{6}Li$(d,\alpha)^4$He, ^{6}Li$(d,p_0)^7$Li, and ^{6}Li$(d,p_1)^7$Li* reactions in the high-energy region. These data should be fitted by the above mentioned parametrized $S_{\text{bare}}(E)$ factors also, i.e., Eq. (5b), as a normalization process,

$$\chi^2 = \sum \frac{[S_{\exp}(E_i) - S_{\text{screen}}(E_i)]^2}{[\Delta S_{\exp}(E_i)]^2}, \tag{5b}$$

where $\Delta S_{\exp}(E_i)$ is the experimental errors reported in the corresponding literature, $S_{\text{screen}}(E_i)$ is the parametrized $S_{\text{bare}}(E)$ multiplied by an enhancement factor with the corresponding screening energy [14]. Since the enhancement effect in the high-energy region is actually negligible compared with that

TABLE I. The extracted parameters for the ^{6}Li$(d,\alpha)^4$He, ^{6}Li$(d,p_0)^7$Li and ^{6}Li$(d,p_1)^7$Li* reactions, respectively.

Parameters	^{6}Li$(d,\alpha)^4$He	^{6}Li$(d,p_0)^7$Li	^{6}Li$(d,p_1)^7$Li*
A		1.05 ± 0.01	
U_s(eV)		478 ± 42	
a (MeV b)	19.20 ± 0.52	20.46 ± 0.63	3.79 ± 0.18
b (b)	-62.24	-56.54	-4.40
c(MeV^{-1} b)	73.13	64.29	0.74
d(MeV^{-2} b)	-29.51	-26.66	1.73

in the low-energy region, e.g., the enhancement is about 0.16% at $E_{\mathrm{c.m.}} = 400$ keV, 29.5% at $E_{\mathrm{c.m.}} = 22.5$ keV, the experimental $S_{\exp}(E)$ in the high-energy region was usually regarded as $S_{\mathrm{bare}}(E)$ approximately.

Finally, all the parameters can be searched for by the goodness test of χ^2 [Eqs. (5a) and (5b), simultaneously] for the six groups' data [three groups of thick-target yields, three groups of reference $S_{\exp}(E)$ points]. In Table I, the values of the parameters are listed, where the common parameters of normalization factor (A) and screening energy (U_s) are 1.05 ± 0.01 and 478 ± 42 eV, respectively. The screening potential $(U_s = 478 \pm 42$ eV$)$ is much larger than the expected value (186 eV) calculated by adiabatic approximation [22]. As we discussed in previous works about the liquid-Li-metal environment (which might be treated as low temperature high density plasma) [31,32], not only the bound electrons but also the conduction electrons and movable Li$^+$ ions would contribute to the screening. Thus, it can be concluded that the present result $(478 \pm 42$ eV$)$ is reasonable.

The measured S-factor values to zero deuteron energy are $S_{\mathrm{bare}}(0) = 19.20 \pm 0.52, 20.46 \pm 0.63$, and 3.79 ± 0.18 MeV b for ^{6}Li$(d,\alpha)^4$He, ^{6}Li$(d,p_0)^7$Li, and ^{6}Li$(d,p_1)^7$Li* reactions respectively. The value of $S_{\mathrm{bare}}(0) = 19.20 \pm 0.52$ MeV b agrees better with the value 18.8 MeV b given by Engstler *et al.* [15] than with the results of other authors

shown in Table II. For the remaining two reactions, however, the present values are much smaller than that estimated by the distorted wave Born approximation (DWBA) [21]. The astrophysical S-factor curves for the three reactions are illustrated in Figs. 3–5. It can be seen from Fig. 3 that the present bare S-factor curve is below the one of Barker, but our S-factor curve and experimental points including the screening potential contribution are higher, because there is a larger screening potential in the liquid Li host. In Ref. [21], Czerski *et al.* estimated two S-factor curves for ^{6}Li$(d,p_0/p_1)^7$Li reactions by DWBA method as shown in Figs. 4 and 5, yet no specific parameters in their original report, which seem to be bare S factor. Obviously, the two curves are larger than the present results.

IV. ASTROPHYSICAL APPLICATIONS

Light element nucleosynthesis is an important chapter of nuclear astrophysics. In order to study the origin and evolution of the light element abundances in the Galaxy, several competing processes should be taken into account, such as the big bang, cosmic ray production, stellar depletion, and nucleosynthesis [33,34]. Stellar nucleosynthesis has yielded most of the Li found today in the interstellar medium of the Galaxy [33].

Generally, the predicted light element depletion strongly depends on the adopted physical inputs, such as the nuclear reaction rates, the equation of state, the opacity of the stellar matter. Nuclear astrophysics reaction rate determines the path of nuclear reactions, thereby affecting the process of stellar evolution. In reaction network calculation, all reactions related to ^{6}Li, ^{7}Li should be taken into account in order to get accurate results.

According to the standard prescription [2], in Figs. 6 and 7 the stellar reaction rates were calculated numerically with the parametrized $S(E)$ factors deduced above. Here, it should be pointed out that the original data measured in this work were far

TABLE II. Comparison of $S_{\mathrm{bare}}(0)$ and U_s for the ^{6}Li$(d,\alpha)^4$He, ^{6}Li$(d,p_0)^7$Li, and ^{6}Li$(d,p_1)^7$Li* reactions, respectively.

		^{6}Li$(d,\alpha)^4$He	^{6}Li$(d,p_0)^7$Li[a]	^{6}Li$(d,p_1)^7$Li*[a]
This work	$S_{\mathrm{bare}}(0)$(MeV b)	19.20 ± 0.52	20.46 ± 0.63	3.79 ± 0.18
	U_s(eV)		478 ± 42[b]	
Czerski *et al.* [21]	$S_{\mathrm{bare}}(0)$(MeV b)		22.6[a]	4.1[a]
	U_s(eV)			
Wang *et al.* [14]	$S_{\mathrm{bare}}(0)$(MeV b)	20.5 ± 0.5		
	U_s(eV)	310 ± 109[c], 218 ± 38[d]		
Engstler *et al.* [15]	$S_{\mathrm{bare}}(0)$(MeV b)	18.8		
	U_s(eV)	380 ± 250[c], 330 ± 120[d]		
Barker [16]	$S_{\mathrm{bare}}(0)$(MeVb)	19.7		
	U_s(eV)	259		
Musumarra *et al.* [20]	$S_{\mathrm{bare}}(0)$(MeVb)	16.9 ± 0.5		
	U_s(eV)	320 ± 50		

[a]No parametrized astrophysical S factor and screening potential for ^{6}Li$(d,p_0/p_1)^7$Li reactions have been found, and the values referred to here are estimated from the curves in Ref. [21].
[b]The three reactions have the same U_s, due to nonisotope dependence [15].
[c]For the LiF solid targets.
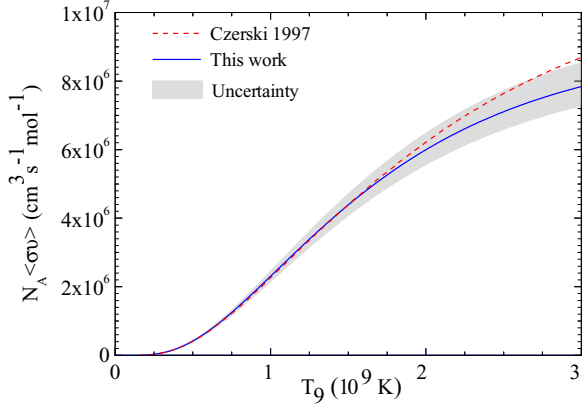[d]For the molecular H_2 or D_2 gas targets, inverse kinematics.

FIG. 6. Stellar reaction rates for the $^6Li(d,\alpha)^4He$ reaction. Dashed curve: Czerski 1997 [37]; solid curve: this work; shadow region: uncertainty of reaction rate.

TABLE III. The extracted parameters for the $^6Li(d,\alpha)^4He$ and $^6Li(d,p_0+p_1)^7Li$ reaction rates, respectively.

Coefficient	$^6Li(d,\alpha)^4He$	$^6Li(d,p_0+p_1)^7Li$
a_1	28.797	29.438
a_2	-0.003	-0.003
a_3	-9.469	-9.512
a_4	-4.538	-5.129
a_5	-0.207	0.651
a_6	0.070	-0.207
a_7	0.339	0.369

below several GK (Gigakelvin) regions. However, combined with the data reported in the high-energy region (>400 keV [15,23]), the reaction rates up to 3 GK were estimated with the deduced $S(E)$ factors. Practically, in order to simplify reaction network calculation, the nuclear astrophysics reaction rate is often fitted as a temperature-related numeric expression. In this work, the fitting formula we adopted is from the JINA Reaclib database [35], and it is expressed as

$$N_A\langle\sigma\upsilon\rangle = \exp\left(a_1 + a_2 T_9^{-1} + a_3 T_9^{-1/3} + a_4 T_9^{1/3}\right.$$
$$\left. + a_5 T_9 + a_6 T_9^{5/3} + a_7 \ln T_9\right), \quad (6)$$

where the coefficients $a_i(i=1,2,3,4,5,6,7)$ are fitting parameters, T_9 is the temperature in 10^9 K, and $N_A\langle\sigma\upsilon\rangle$ is the reaction rate in cm^3 s^{-1} mol^{-1}. The process parametrization is achieved

through the evaluation tool, Computational Infrastructure for Nuclear Astrophysics [36]. In Table III, the optimized parameters of Eq. (6) for these reactions were listed, where the uncertainty for each parameter transferred from the deduced $S(E)$ factors was not definitely indicated. Instead of that, the upper and lower bounds of reaction rates for these reactions were estimated from the uncertainties of $S(E)$ curves. For the $^6Li(d,\alpha)^4He$ reaction, the relative uncertainty changed from $\binom{+2.8\%}{-3.9\%}$ to $\binom{+8.8\%}{-7.2\%}$; for the $^6Li(d,p_0+p_1)^7Li$ reaction, the relative uncertainty changed from $\binom{+4.2\%}{-5.9\%}$ to $\binom{+7.0\%}{-13.1\%}$ as the temperature changed in the 0.01–3 GK region. More details were shown as the shadow region in Figs. 6 and 7.

According to the reports [7,18] about two more important reactions, i.e., $^6Li(p,^3He)^4He$ and $^7Li(p,\alpha)^4He$ reactions [38], we can easily predict that the variation here in the astrophysics reaction rates for the $^6Li(d,\alpha/p)$ reactions are not expected to produce an obvious change in the current astrophysical scenarios. However, it seems still worthwhile to investigate the effect of the new values on the lithium abundance and the importance for the two reactions in stellar element synthesis.

In order to achieve these purposes, we calculated the abundances of ^6Li and ^7Li in solar proton-proton burning, and the difference of several simulations lie in the astrophysics reaction rates for the $^6Li(d,\alpha/p)$ reactions. The behaviors of ^6Li and ^7Li abundances as a function of time during the solar proton-proton burning are shown in Fig. 8 which actually
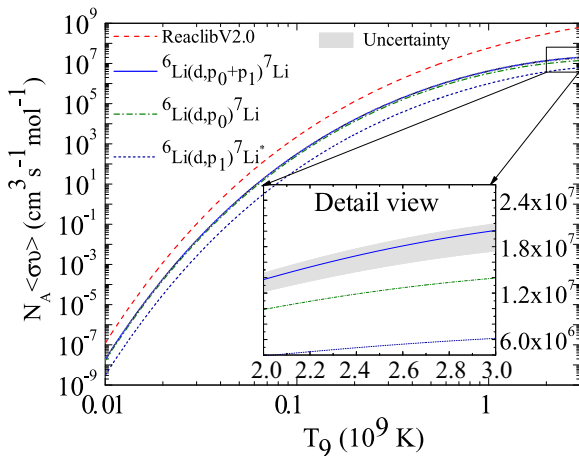

FIG. 7. Stellar reaction rates for the $^6Li(d,p)^7Li$ reaction. The dashed curve represents the rate of ReaclibV2.0 [35]. The dashed-dotted and short dashed curves are the rate of $^6Li(d,p_0)^7Li$ and $^6Li(d,p_1)^7Li$ reactions, respectively, which are obtained based on the present work. The solid curve is the total contribution of the two reactions, with the shadow region (as detailed shown in the inset) corresponding to the uncertainty of reaction rate.
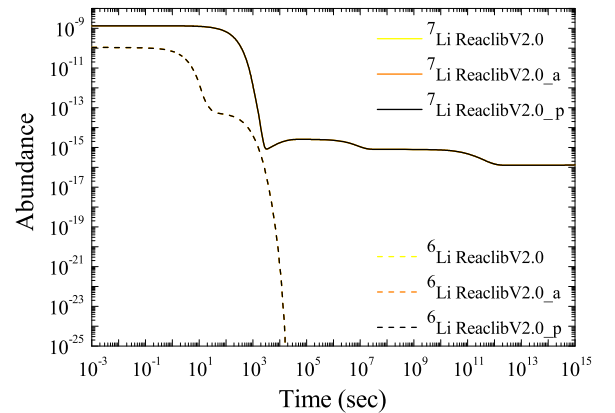

FIG. 8. The behaviors of ^6Li and ^7Li abundances in solar proton-proton burning. Six simulations were included, though there seem to be only two curves due to overlapping.

includes many simulations, though there seem to be only two curves.

We used the astrophysics reaction rates of several different rate libraries to simulate the abundance of ^{6}Li and ^{7}Li. The first one is the rate library ReaclibV2.0 [35] which does not include the ^{6}Li$(d,\alpha)^4$He reaction; the second one, i.e., ReaclibV2.0_a is a new rate library which adds our result of the ^{6}Li$(d,\alpha)^4$He reaction on the basis of ReaclibV2.0; the last one, i.e., ReaclibV2.0_p is a new rate library which has taken the place of the original ^{6}Li$(d,p)^7$Li reaction rate of ReaclibV2.0 with our own result. Unfortunately, as shown in Fig. 8, despite the use of different simulation conditions, no changes are found after adding the ^{6}Li$(d,\alpha)^4$He reaction rate or replacing the ^{6}Li$(d,p)^7$Li reaction rate. According to what has just been described, predictably, the uncertainties of reaction rates would cause no issue for simulation results. At the same time, our numerical results verify this conjecture, though the results were not represented in Fig. 8.

Therefore, we may conclude that there is almost no effect for ^{6}Li$(d,\alpha)^4$He and ^{6}Li$(d,p)^7$Li reactions on the abundance of ^{6}Li and ^{7}Li, based on this measurement with the low energy limit ($E_{\text{lab}} = 30$ keV). They may not play a key role in stellar element synthesis, unless there is an undiscovered mechanism, i.e., resonance reactions, or abnormal enhancement in the ultralow-energy region. In previous work, Pizzone $et\ al.$ [18] reported a similar conclusion to ours. They measured the ^{6}Li$(p,\alpha)^3$He bare nucleus cross section at astrophysical energies in the framework of the Trojan-horse method (THM), and investigated the variation of ^{6}Li and ^{7}Li abundances in the premain sequence (PMS) phase. So far, lithium abundance might be a problem in astrophysics and needs us to improve our knowledge of the mixing mechanism, and to improve the accuracy of observation data. Meanwhile, many other mechanisms

have been suggested to solve the "lithium problem" also, i.e., the presence of negatively charged weak-scale particles [39], undiscovered light electrically neutral particles [40].

V. CONCLUSIONS

In this work, the screening potential and their respective astrophysical $S(E)$ factors of the ^{6}Li$(d,\alpha)^4$He, ^{6}Li$(d,p_0)^7$Li, and ^{6}Li$(d,p_1)^7$Li* reactions have been extracted, combined with literature data. Different from previous works in which three reactions were investigated independently, we fit them simultaneously, based on the fact that the screening effects depend on the environments and the three reactions have the same screening energy. The deduced screening potential value $U_s = 478 \pm 42$ eV is larger than the expected value of 186 eV calculated by adiabatic approximation.

In addition we have determined the stellar reaction rates for the ^{6}Li$(d,\alpha)^4$He and ^{6}Li$(d,p_0 + p_1)^7$Li reactions for temperatures up to $T = 3 \times 10^9$ K, with the combined data set in the high-energy region reported in previous works. Therefore, we estimated the abundances of isotopes ^{6}Li and ^{7}Li in solar proton-proton burning, which resulted in almost no effect for ^{6}Li$(d,\alpha)^4$He and ^{6}Li$(d,p)^7$Li reactions on the abundance of ^{6}Li and ^{7}Li, based on the data set measured in the above mentioned energy region.

[1] S. Ichimaru, Rev. Mod. Phys. **54**, 1017 (1982).

[2] C. Rolfs and W. Rodney, *Cauldrons in the Cosmos: Nuclear Astrophysics* (University of Chicago Press, Chicago, 1988).

[3] D. L. Lambert, AIP Conf. Proc. **743**, 206 (2004).

[4] B. D. Fields, Annu. Rev. Nucl. Part. Sci. **61**, 47 (2011).

[5] M. Asplund, D. L. Lambert, P. E. Nissen, F. Primas, and V. V. Smith, Astrophys. J. **644**, 229 (2006).

[6] M. Asplund and J. Meléndez, AIP Conf. Proc. **990**, 342 (2008).

[7] R. G. Pizzone, C. Spitaleri, M. Lattuada, S. Cherubini, A. Musumarra, M. G. Pellegriti, S. Romano, A. Tumino, V. Castellani, S. Degl'Innocenti, and A. Imperio, Astron. Astrophys. **398**, 423 (2003).

[8] C. Rolfs, Prog. Part. Nucl. Phys. **59**, 43 (2007).

[9] H. J. Assenbaum, K. Langanke, and C. Rolfs, Z. Physik A: At. Nucl. **327**, 461 (1987).

[10] F. Raiola, L. Gang, C. Bonomo, G. Gyürky, M. Aliotta, H. W. Becker, R. Bonetti, C. Broggini, P. Corvisiero, A. D'Onofrio, Z. Fülöp, G. Gervino, L. Gialanella, M. Junker, P. Prati, V. Roca, C. Rolfs, M. Romano, E. Somorjai, F. Strieder, F. Terrasi, G. Fiorentini, K. Langanke, and J. Winter, Eur. Phys. J. A **19**, 283 (2004).

[11] C. Kittel, *Introduction to Solid State Physics*, 6th ed. (Wiley, New York, 1986).

[12] J. N. Bahcall, L. S. Brown, A. Gruzinov, and R. F. Sawyer, Astron. Astrophys. **383**, 291 (2002).

[13] J. Kasagi, Prog. Theor. Phys. Suppl. **154**, 365 (2004).

[14] T. S. Wang, X. C. Guan, K. H. Fang, J. T. Zhao, Q. H. He, M. C. Lan, and X. X. Xu, J. Phys. G: Nucl. Part. Phys. **39**, 015201 (2012).

[15] S. Engstler, G. Raimann, C. Angulo, U. Greife, C. Rolfs, U. Schröder, E. Somorjai, B. Kirch, and K. Langanke, Z. Phys. A **342**, 471 (1992).

[16] F. C. Barker, Nucl. Phys. A **707**, 277 (2002).

[17] J. Cruz, Z. Fulop, G. Gyurky, F. Raiola, A. Leva, B. Limata, M. Fonseca, H. Luis, D. Schurmann, M. Aliotta, H. W. Becker, A. P. Jesus, K. U. Kettner, J. P. Ribeiro, C. Rolfs, M. Romano, E. Somorjai, and F. Strieder, Phys. Lett. B **624**, 181 (2005).

[18] R. G. Pizzone, A. Tumino, S. D. Innocenti, C. Spitaleri, S. Cherubini, A. Musumarra, and S. Romano, Astron. Astrophys. **438**, 779 (2005).

[19] R. G. Pizzone, C. Spitaleri, M. Lattuada, A. Musumarra, M. G. Pellegriti, S. Romano, A. Tumino, S. Cherubini, P. Figuera, D. Miljanic, C. Rolfs, S. Typel, H. H. Wolter, V. Castellani, S. D. Innocenti, and A. Imperio, Nucl. Phys. A **718**, 496c (2003).

[20] A. Musumarra, R. G. Pizzone, S. Blagus, M. Bogovac, P. Figuera, M. Lattuada, M. Milin, D. Miljanic, M. G. Pellegriti,

D. Rendic, C. Rolfs, N. Soic, C. Spitaleri, S. Typel, H. H. Wolter, and M. Zadro, Phys. Rev. C **64**, 068801 (2001).

[21] K. Czerski, H. Bucka, P. Heide, and T. Makubire, Phys. Lett. B **307**, 20 (1993).

[22] L. Bracci, G. Fiorentini, V. S. Melezhik, G. Mezzorani, and P. Quarati, Nucl. Phys. A **513**, 316 (1990).

[23] A. J. Elwyn, R. E. Holland, C. N. Davids, L. Meyer-Schutzmeister, J. E. Monahan, F. P. Mooring, and W. Ray, Phys. Rev. C **16**, 1744 (1977).

[24] G. Baur, Phys. Lett. B **178**, 135 (1986).

[25] Y. Yuki, T. Sato, T. Ohtsuki, T. Yorita, Y. Aoki, H. Yamazaki, J. Kasagi, and K. Ishii, J. Phys. Soc. Jpn. **66**, 73 (1997).

[26] Y. Toriyabe, E. Yoshida, J. Kasagi, and M. Fukuhara, Phys. Rev. C **85**, 054620 (2012).

[27] K. H. Fang, J. X. Zou, E. Yoshida, T. S. Wang, and J. Kasagi, Europhys. Lett. **109**, 22002 (2015).

[28] J. T. Zhao, Q. Wang, D. D. Liu, Z. H. Wang, K. H. Fang, T. S. Wang, and J. Kasagi, Nucl. Instrum. Methods Phys. Res. B **360**, 139 (2015).

[29] H. Jeremie, P. Martin, and A. Calamand, Nucl. Phys. A **105**, 689 (1967).

[30] J. F. Ziegler and J. P. Biersack, SRIM code, http://www.srim.org.

[31] J. Kasagi and H. Yonermura, AIP Conf. Proc. **1098**, 161 (2009).

[32] K. H. Fang, T. S. Wang, H. Yonemura, A. Nakagawa, T. Sugawara, and J. Kasagi, J. Phys. Soc. Jpn. **80**, 084201 (2011).

[33] L. M. Hobbs, Phys. Rep. **333**, 449 (2000).

[34] E. Vangioni-Flam, M. Casse, and J. Audouze, Phys. Rep. **333**, 365 (2000).

[35] https://groups.nscl.msu.edu/jina/reaclib/db/index.php

[36] http://nucastrodata.org/infrastructure.html

[37] K. Czerski, A. Huke, H. Bucka, P. Heide, G. Ruprecht, and B. Unrau, Phys. Rev. C **55**, 1517 (1997).

[38] P. D. Serpico, S. Esposito, F. Iocco, G. Mangano, G. Miele, and O. Pisanti, J. Cosmol. Astropart. Phys. **12**, 010 (2004).

[39] M. Kusakabe, K. S. Kim, M. K. Cheoun, T. Kajino, Y. Kino, and G. J. Mathews, Astrophys. J. Suppl. Ser. **214**, 5 (2014).

[40] A. Goudelis, M. Pospelov, and J. Pradler, Phys. Rev. Lett. **116**, 211303 (2016).